

# OPTIMIZATION OF INJECTION MOLDING QUALITY BASED ON BP NEURAL NETWORK AND PSO

## OPTIMIZACIJA KVALITETE INJEKCIJSKEGA BRIZGANJA NA OSNOVI NEVRONSKIH MREŽ IN ALGORITMA OPTIMIZACIJE Z ROJEM DELCEV

Feng Lin<sup>1</sup>, Jingying Duan<sup>2</sup>, Qiuxia Lu<sup>2</sup>, Xibing Li<sup>3,4,\*</sup>

<sup>1</sup>Fuzhou Polytechnic, College of Mechanical and Electronic Engineering, Fuzhou, China

<sup>2</sup>Shandong Labor Vocational and Technology College, Jinan, China

<sup>3</sup>Fujian Agriculture and Forestry University, College of Mechanical and Electronic Engineering, Fuzhou, China

<sup>4</sup>Fujian Key Laboratory of Agricultural Information Sensing Technology, Fuzhou, China

*Prejem rokopisa – received: 2022-06-08; sprejem za objavo – accepted for publication: 2022-07-25*

doi:10.17222/mit.2022.516

An electronic product shell is prone to uneven shrinkage, warpage and sink marks, resulting in a large number of unqualified products and increased costs. Therefore, volumetric shrinkage, warpage deformation and sink mark index are selected as optimization goals. Based on the orthogonal test and entropy weight method, a multi-objective optimization was transformed into a comprehensive evaluation optimization. A BP neural network combined with a particle swarm optimization algorithm was used to obtain the optimal combination of process parameters, simulated by Moldflow to reduce volumetric shrinkage to 3.46 %, warpage deformation to 2.538 mm, and the sink mark index to 1.87 % so as to improve the injection molding quality of the plastic parts and meet the requirements of qualified parts. The combination of the BP neural network and particle swarm optimization algorithm can prevent the defects such as large shrinkage, warpage and sink marks.

Keywords: orthogonal test, entropy weight, neural network, particle swarm optimization

Plastična ohišja elektronskih izdelkov so med postopkom injekcijskega brizganja nagnjena k neenakomernemu krčenju, ukrivljanju in izgubljanju napisov ali oznak oz. potencialnemu krčenju zaradi vroče sredice (SMI; angl.: sink mark index), kar privede do nastanka nekakovostnih izdelkov in povečanja stroškov. Zaradi tega so se avtorji članka posvetili optimizaciji volumskih skrčkov, deformacij zaradi krivljenja in krčenju zaradi vroče sredice. Na osnovi ortogonalnih testov in metode analize entropije (angl.: entropy weight method) so več objektno optimizacijo transformirali v obsežno optimizacijsko ovrednotenje. Z uporabo kombinacije metod povratno napredovanih (BP; angl.: back propagation) nevronske mreže in algoritma optimizacije z rojem delcev (PSO; angl.: particle swarm optimization) so dobili optimalno kombinacijo procesnih parametrov, ki so jih simulirali s programskim orodjem Moldflow in tako zmanjšali volumski skrček na 3,46 %, deformacijo zaradi ukrivljanja na 2,538 mm in krčenje zaradi vroče sredice na 1,87 %. S tem so izboljšali kakovost procesa injekcijskega brizganja plastičnih izdelkov in dosegli zahtevano kakovost le-teh. Pokazali so, da uporaba kombinacije metod povratno napredovanih nevronske mreže in algoritma optimizacije z rojem delcev lahko pomaga pri reševanju napak kot so razne deformacije in krivljenja, ki nastajajo med postopkom injekcijskega brizganja plastičnih ohišij za elektronske sestavne dele.

Ključne besede: ortogonalni test, analiza entropije, nevronske mreže, optimizacija z rojem delcev

## 1 INTRODUCTION

### 1.1 General

With the advent of the intelligent era, electronic products began to be applied extensively. The speed of the renewal of plastic housings for electronic products is accelerating, placing higher demand on the quality of plastic parts. The quality of injection plastic parts is jointly determined by the injection process parameters and mold structure. By optimizing the injection process parameters, quality defects of plastic parts such as warpage deformation can be avoided.<sup>1</sup> By replacing repeated test molds with reasonable orthogonal experimental design and Moldflow numerical simulation technology, Y. Nie et al. obtained optimized injection process parameters based on a range analysis and variance analysis

instead.<sup>2-4</sup> G. Xu et al. studied the impact of injection process parameters on the multi-objective quality of plastic parts using orthogonal experimental design, signal-to-noise ratio calculation and gray correlation analysis, and then obtained the optimal combination of process parameters.<sup>5-7</sup> H. G. Zhang et al. transformed a multi-objective optimization problem into a single-objective optimization problem based on the entropy weight method and obtained the optimal process parameter combination through a comprehensive evaluation.<sup>8,9</sup>

In the present work, an electronic product backshell was selected as the object of study. Based on the numerical simulation technology (Moldflow) and orthogonal test, the entropy weight method was introduced to get the test data. Then, a back propagation (BP) neural network model was established using Python to find a better combination of the process parameters through global optimization of the particle swarm optimization algorithm.

\*Corresponding author's e-mail:  
lxbwj@163.com (Xibing Li)

### 1.2 3D model and mesh division of the back cover of an electronic product

The 3D model of the backshell of this electronic product is shown in **Figure 1**. The maximum size of the backshell is  $(376 \times 308 \times 45)$  mm, with the average wall thickness of 2.25 mm. The material is an acrylonitrile-butadiene-styrene copolymer, named ABS. It has a good overall performance with the recommended range of parameters: mold temperature (40–70 °C), melt temperature (190–220 °C), holding pressure (65–95 MPa), pressure holding time (6–12 s), injection pressure (70–130 MPa) and injection time (0.9–1.3 s).

The backshell of the electronic product has four convex platform holes and many reinforcement plates, and there are square holes on the sides. The product structure is complex and prone to quality defects such as deformation and uneven shrinkage after molding. Meanwhile, the structure of the plastic part has many features such as chamfers and edges, which are favorable to injection molding, but unfavorable to the mesh division of a numerical simulation. The CADdoctor2018 software was used to simplify the structure of the 3D model of the product, and then the file was imported into Moldflow2019 for a mesh division. The plastic part is thin-walled, with a uniform wall thickness. Using a double-layer grid, the average aspect ratio of the grid is 2.12, the match percentage is 91.2 % and the reciprocal percentage is 91.3 %, meeting the requirements of the double-layer-grid numerical-simulation analysis.

The sequence analysis of the fill pressure warp was selected. At the recommended mold temperature of 50 °C, melt temperature of 205 °C and other default parameters, the volumetric shrinkage obtained by the Moldflow simulation was 5.57 %, the warpage deformation was 2.563 mm and the sink mark index was 3.57 %. However, a qualified injection product needs to have a volumetric shrinkage of less than 4.5 %, a maximum warpage deformation of less than 3 mm and as small as possible, and no sink marks if possible. When an injection mold structure has been determined, the injection

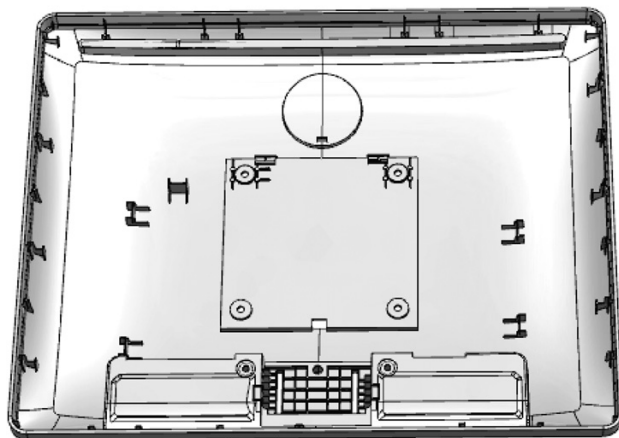


**Figure 1:** 3D model of the back cover of the electronic product

process parameters should be optimized to reduce the volumetric shrinkage, warpage deformation and sink mark index in order to improve the yield.

## 2 EXPERIMENTAL PART

### 2.1 Orthogonal experimental design

According to the orthogonal experimental design, the volumetric shrinkage, warpage deformation and sink mark index were selected as experimental targets. According to the molding characteristics of the ABS material, the mold temperature, melt temperature, holding pressure, pressure-holding time, injection pressure and injection time were selected as the experimental factors. Four levels were selected for each factor, as shown in **Table 1**.<sup>10,11</sup> An L32 (4<sup>6</sup>) orthogonal array test table was adopted, and the orthogonal test design and simulation results are shown in **Table 2**.

**Table 1:** Table of the orthogonal-test factor levels

| Level | Factor |      |       |     |       |     |
|-------|--------|------|-------|-----|-------|-----|
|       | A/°C   | B/°C | C/MPa | D/s | E/MPa | F/s |
| 1     | 40     | 190  | 95    | 6   | 70    | 0.9 |
| 2     | 50     | 200  | 85    | 8   | 90    | 1.1 |
| 3     | 60     | 210  | 75    | 10  | 110   | 1.3 |
| 4     | 70     | 220  | 65    | 12  | 130   | 1.5 |

A – mold temperature (°C), B – melt temperature (°C), C – holding pressure (MPa), D – pressure-holding time (s), E – injection pressure (MPa), F – injection time (s), numbers 1–4 indicate the level of each test factor

**Table 2:** Orthogonal experimental design and simulation results

| Test No. | A/°C | B/°C | C/MPa | D/s | E/MPa | F/s | Y <sub>1</sub> /% | Y <sub>2</sub> /mm | Y <sub>3</sub> /% |
|----------|------|------|-------|-----|-------|-----|-------------------|--------------------|-------------------|
| 1        | 40   | 190  | 95    | 6   | 70    | 0.9 | 4.742             | 2.606              | 2.716             |
| 2        | 40   | 200  | 85    | 8   | 90    | 1.1 | 6.985             | 2.473              | 2.748             |
| 3        | 40   | 210  | 75    | 10  | 110   | 1.3 | 8.3               | 2.821              | 3.333             |
| 4        | 40   | 220  | 65    | 12  | 130   | 1.5 | 8.751             | 2.878              | 3.794             |
| 5        | 50   | 190  | 95    | 8   | 90    | 1.3 | 6.807             | 2.457              | 2.468             |
| 6        | 50   | 200  | 85    | 6   | 70    | 1.5 | 6.93              | 2.54               | 3.484             |
| 7        | 50   | 210  | 75    | 12  | 130   | 0.9 | 5.311             | 2.703              | 3.017             |
| 8        | 50   | 220  | 65    | 10  | 110   | 1.1 | 8.646             | 2.789              | 3.628             |
| 9        | 60   | 190  | 85    | 10  | 130   | 0.9 | 4.965             | 2.669              | 2.549             |
| 10       | 60   | 200  | 95    | 12  | 110   | 1.1 | 4.45              | 2.371              | 2.607             |
| 11       | 60   | 210  | 65    | 6   | 90    | 1.3 | 6.038             | 2.922              | 4.166             |
| 12       | 60   | 220  | 75    | 8   | 70    | 1.5 | 7.545             | 2.425              | 4.309             |
| 13       | 70   | 190  | 85    | 12  | 110   | 1.3 | 5.625             | 2.575              | 2.514             |
| 14       | 70   | 200  | 95    | 10  | 130   | 1.5 | 7.649             | 2.292              | 3.222             |
| 15       | 70   | 210  | 65    | 8   | 70    | 0.9 | 7.621             | 5.520              | 4.427             |
| 16       | 70   | 220  | 75    | 6   | 90    | 1.1 | 8.744             | 2.469              | 4.72              |
| 17       | 40   | 190  | 65    | 6   | 130   | 1.1 | 6.423             | 3.119              | 3.666             |
| 18       | 40   | 200  | 75    | 8   | 110   | 0.9 | 7.818             | 2.852              | 3.019             |
| 19       | 40   | 210  | 85    | 10  | 90    | 1.5 | 7.867             | 2.536              | 2.774             |
| 20       | 40   | 220  | 95    | 12  | 70    | 1.3 | 5.643             | 2.537              | 2.866             |
| 21       | 50   | 190  | 65    | 8   | 110   | 1.5 | 6.062             | 3.201              | 3.872             |
| 22       | 50   | 200  | 75    | 6   | 130   | 1.3 | 7.702             | 2.851              | 3.427             |
| 23       | 50   | 210  | 85    | 12  | 70    | 1.1 | 5.148             | 2.532              | 2.781             |
| 24       | 50   | 220  | 95    | 10  | 90    | 0.9 | 5.364             | 2.301              | 3.577             |

|    |    |     |    |    |     |     |       |       |       |
|----|----|-----|----|----|-----|-----|-------|-------|-------|
| 25 | 60 | 190 | 75 | 10 | 70  | 1.1 | 5.717 | 3.985 | 3.936 |
| 26 | 60 | 200 | 65 | 12 | 90  | 0.9 | 7.129 | 5.46  | 5.172 |
| 27 | 60 | 210 | 95 | 6  | 110 | 1.5 | 8.326 | 2.353 | 4.013 |
| 28 | 60 | 220 | 85 | 8  | 130 | 1.3 | 9.055 | 2.407 | 4.249 |
| 29 | 70 | 190 | 75 | 12 | 90  | 1.5 | 6.311 | 6.583 | 4.079 |
| 30 | 70 | 200 | 65 | 10 | 70  | 1.3 | 6.643 | 4.694 | 4.605 |
| 31 | 70 | 210 | 95 | 8  | 130 | 1.1 | 8.365 | 2.216 | 3.977 |
| 32 | 70 | 220 | 85 | 6  | 110 | 0.9 | 8.486 | 2.270 | 4.667 |

In **Table 2**,  $Y_1$ ,  $Y_2$  and  $Y_3$  represent the volumetric shrinkage (%), warpage deformation (mm) and sink mark index (%).

## 2.2 Analysis of the single-objective optimization result

Through the orthogonal test, the experiment result that minimizes the single target in 32 sets could be found, but the combination of injection process parameters could not be optimized. The range analysis allows us to find the optimal combination of process parameters and the ranking of the degree of influence of the process parameters on the target.<sup>12,13</sup> A statistical analysis was conducted on the test results from **Table 2** to obtain the mean value of each level of volumetric shrinkage and the range analysis was used for the factors, as shown in **Table 3**.

As shown in **Table 3**, for the volumetric shrinkage, the optimal process parameter combination is A2-B1-C1-D4-E1-F1, i.e., the mold temperature is 50 °C, the melt temperature is 190 °C, the holding pressure is 95 MPa, the pressure-holding time is 12 s, the injection pressure is 70 MPa and the injection time is 0.9 s. Moldflow was used for the numerical simulation; the optimized volumetric shrinkage was 4.02 % and the sink mark index was 2.14 %, but the warpage deformation was 2.573 mm, which was not optimized.

Consequently, the following conclusions could be drawn. For the warpage deformation, the optimal combination of process parameters is A2-B4-C1-D1-E4-F2. The optimized warpage deformation was 2.154 mm, but the volumetric shrinkage was 8.49 %, and the sink mark index was 4.36 %. The volumetric shrinkage and sink mark index were not optimized. For the sink mark index, the best combination of process parameters is A1-B1-C1-D4-E3-F3. The optimized sink mark index was 2.43 %, but the volumetric shrinkage was 7.07 %

and the warpage deformation was 2.597 mm. The volumetric shrinkage and warpage deformation were not optimized. The injection molding process parameters of the backshell of this electronic product have different degrees of influence on the volumetric shrinkage, warpage deformation and sink mark index, so the optimization of multiple objectives could not be achieved simultaneously.

## 2.3 Comprehensive assessment

Considering that volumetric shrinkage, sink mark index and warpage deformation have different effects on a comprehensive evaluation of products, the entropy weight method was introduced to determine the weight of each index and convert the multi-objective optimization problem into a single-objective comprehensive evaluation problem.<sup>14-16</sup> In order to eliminate the effect of different dimensions, it is necessary to normalize all the indicators. As smaller values of all the indicators are better, negative indicators are adopted for the normalization, and the formula is shown below:

$$Y_{ij}^* = \frac{\max(Y_j) - Y_{ij}}{\max(Y_j) - \min(Y_j)} \quad (1)$$

In Equation (1),  $j = 1-3$ ,  $I = 1-32$ ,  $Y_{ij}^*$  represents the  $i$ -th sample of the  $j$ -th indicator,  $\max(Y_j)$  is the maximum value of the  $j$ -th indicator and  $\min(Y_j)$  is the minimum value of the  $j$ -th indicator. After the normalization, a data normalization table was obtained as shown in **Table 4**. Then the entropy value was calculated based on the normalized evaluation index, and the entropy value  $e_j$  of the  $j$ -th evaluation index is shown in Equation (2).

$$e_j = -\frac{1}{n} \sum_{i=1}^n \frac{Z_{ij}}{\sum_{i=1}^n Z_{ij}} \ln \frac{Z_{ij}}{\sum_{i=1}^n Z_{ij}} \quad (2)$$

In Equation (2),  $n = 32$ , and when

$$Z_{ij} = 0, \quad \ln \frac{Z_{ij}}{\sum_{i=1}^n Z_{ij}} = 0$$

Finally, the corresponding weight coefficient was calculated in accordance with the entropy value. The weight coefficient of the  $j$ -th evaluation index is shown in Equa-

**Table 3:** Range analysis table for the volumetric shrinkage from the orthogonal test

| Level            | A – mold temperature (°C) | B – melt temperature (°C) | C – holding pressure (MPa) | D – pressure holding time (s) | E – injection pressure (MPa) | F – injection time (s) |
|------------------|---------------------------|---------------------------|----------------------------|-------------------------------|------------------------------|------------------------|
| 1                | 7.0661                    | <b>5.8315</b>             | <b>6.4183</b>              | 7.1739                        | <b>6.2486</b>                | <b>6.4295</b>          |
| 2                | <b>6.4963</b>             | 6.9133                    | 6.8826                     | 7.5323                        | 6.9057                       | 6.8098                 |
| 3                | 6.6531                    | 7.1220                    | 7.1810                     | 6.8939                        | 7.2141                       | 6.9766                 |
| 4                | 7.4305                    | 7.7793                    | 7.1641                     | <b>6.0460</b>                 | 7.2776                       | 7.4301                 |
| Range            | 0.9342                    | 1.9478                    | 0.7627                     | 1.4863                        | 1.0290                       | 1.0006                 |
| Influence degree | 5                         | 1                         | 6                          | 2                             | 3                            | 4                      |
| Best combination | 50                        | 190                       | 95                         | 12                            | 70                           | 0.9                    |

tion (3), and the weight coefficients of volumetric shrinkage, warpage deformation and sink mark index were 0.533, 0.159 and 0.308, respectively. In accordance with Equation (4), weighted comprehensive evaluation scores were calculated as shown in **Table 4**.

$$W_j = \frac{1 - e_j}{\sum_{j=1}^3 1 - e_j} \quad (3)$$

$$Z_i = (Y_{i1} W_1 + Y_{i2} W_2 + Y_{i3} W_3) \times 100 \quad (4)$$

**Table 4:** Normalized data standardization table and comprehensive evaluation scores

| Test No. | $Y_1^*$ | $Y_2^*$ | $Y_3^*$ | Comprehensive evaluation scores $Z_i$ | Sorting |
|----------|---------|---------|---------|---------------------------------------|---------|
| 1        | 0.9366  | 0.9107  | 0.9083  | 92.3672                               | 2       |
| 2        | 0.4495  | 0.9411  | 0.8964  | 66.6724                               | 10      |
| 3        | 0.1640  | 0.8615  | 0.6801  | 43.5561                               | 21      |
| 4        | 0.0660  | 0.8484  | 0.5096  | 32.8714                               | 27      |
| 5        | 0.4882  | 0.9448  | 1.0000  | 71.9898                               | 9       |
| 6        | 0.4615  | 0.9258  | 0.6243  | 58.6221                               | 15      |
| 7        | 0.8130  | 0.8885  | 0.7970  | 82.0123                               | 6       |
| 8        | 0.0888  | 0.8688  | 0.5710  | 36.3091                               | 26      |
| 9        | 0.8882  | 0.8963  | 0.9700  | 91.4844                               | 3       |
| 10       | 1.0000  | 0.9645  | 0.9486  | 97.8385                               | 1       |
| 11       | 0.6552  | 0.8383  | 0.3720  | 59.6700                               | 14      |
| 12       | 0.3279  | 0.9521  | 0.3192  | 42.5071                               | 22      |
| 13       | 0.7448  | 0.9178  | 0.9830  | 84.6340                               | 5       |
| 14       | 0.3053  | 0.9826  | 0.7212  | 54.2593                               | 17      |
| 15       | 0.3114  | 0.2434  | 0.2755  | 28.9399                               | 28      |
| 16       | 0.0675  | 0.9421  | 0.1672  | 23.8344                               | 32      |
| 17       | 0.5716  | 0.7932  | 0.5570  | 60.2494                               | 13      |
| 18       | 0.2686  | 0.8544  | 0.7962  | 52.5898                               | 18      |
| 19       | 0.2580  | 0.9267  | 0.8868  | 55.9924                               | 16      |
| 20       | 0.7409  | 0.9265  | 0.8528  | 80.5305                               | 7       |
| 21       | 0.6499  | 0.7744  | 0.4808  | 61.7421                               | 12      |
| 22       | 0.2938  | 0.8546  | 0.6453  | 49.2510                               | 19      |
| 23       | 0.8484  | 0.9276  | 0.8842  | 87.2204                               | 4       |
| 24       | 0.8015  | 0.9805  | 0.5899  | 76.4550                               | 8       |
| 25       | 0.7249  | 0.5949  | 0.4571  | 62.1066                               | 11      |
| 26       | 0.4182  | 0.2572  | 0.0000  | 26.2813                               | 30      |
| 27       | 0.1583  | 0.9686  | 0.4286  | 37.1756                               | 25      |
| 28       | 0.0000  | 0.9563  | 0.3413  | 25.8819                               | 31      |
| 29       | 0.5959  | 0.0000  | 0.4042  | 44.1120                               | 20      |
| 30       | 0.5238  | 0.4326  | 0.2097  | 41.1816                               | 23      |
| 31       | 0.1498  | 1.0000  | 0.4419  | 37.6414                               | 24      |
| 32       | 0.1236  | 0.9876  | 0.1868  | 28.1405                               | 29      |

### 3 PROCESS PARAMETER OPTIMIZATION AND VALIDATION

#### 3.1 Comprehensive evaluation and analysis

According to the ranking of comprehensive evaluation scores from **Table 4**, test No. 10 had the highest comprehensive evaluation score. In order to further analyze the significant impacts of process parameters on the comprehensive evaluation indexes and determine the op-

timal process parameters, the range analysis was used to analyze the comprehensive evaluation scores from **Table 4**. The order of the influence of each process parameter on the comprehensive evaluation index was  $B > C > A > D > F > E$ . The optimal process parameter combination was A2-B1-C1-D4-E1-F1, which was the same as the optimal process parameter combination of the minimum volumetric shrinkage. Compared with the test result for No. 10, the volumetric shrinkage was reduced by about 9.6 %, the sink mark index was reduced by about 18 %, while the warpage deformation increased. However, due to the small weight proportion, the warpage deformation had little influence on the comprehensive evaluation. Therefore, according to the comprehensive evaluation, the overall quality of the plastic part was improved.

#### 3.2 BP-PSO process parameter optimization

To find a better combination of injection process parameters, a BP neural network was used to fit the input-output relationship model, and the optimal value of the model was obtained with the particle swarm optimization algorithm.

##### 3.2.1 Establishing an input-output relationship prediction model based on the BP neural network

The BP neural network is a classical error feed-forward neural network, widely used in scientific research fields due to its multi-dimensional nonlinear mapping capability.<sup>17–19</sup> In terms of the structure, this work adopted a four-layer BP neural network model. The input layer had 6 nodes, the second hidden layer had 11 nodes, the third hidden layer had 11 nodes, and there were 3 nodes in the output layer of the model. The 6 process parameters and the comprehensive evaluation were taken as the input and output of the BP neural network. 90 % of the 32 sets of orthogonal test data was randomly selected as the training data, and the rest was used as the test data set. Before training the neural network, the input and output data were normalized with Equation (5). The Keras library of Python was used to build the BP neural-network framework. The `tb.keras.regularizers.l2` method was used for the hidden layer to avoid over-fitting, and then it was activated with the Relu function. The loss function was MSE.

$$x^* = \frac{X_{ij} - \min(X_j)}{\max(X_j) - \min(X_j)} \quad (5)$$

After 2000 iterations, the evaluation indexes were as follows:  $\text{mae} = 0.0457$ ,  $\text{mse} = 0.004$ ,  $\text{val\_mae} = 0.0587$  and  $\text{val\_mse} = 0.0055$ . After the training of the BP neural network, the predicted values of the comprehensive evaluation scores were obtained, and the predicted values were compared with the real values as shown in **Figure 2**. It can be seen from this figure that the real values and predicted values of the comprehensive evaluation re-





**Figure 2:** Comparison between the real values and predicted values of the training set

mained largely consistent, although there were errors. The BP neural network model obtained reflects the relationship between the input and output very well.

The remaining data set was used for the test. The real values of the comprehensive evaluation scores (36.3091, 92.3672, 82.0123) for the test set were basically consistent with the predicted values (37.8348, 88.2714, 74.5526). This proved that the established BP neural network model was feasible.

### 3.2.2 Optimization of process parameters based on PSO

The PSO algorithm, i.e., the particle swarm optimization algorithm, is an intelligent optimization algorithm that simulates the foraging behavior of a flock of birds and optimizes the flock with the information exchange among the individuals of the flock.<sup>20,21</sup> The negative value of comprehensive evaluation score  $Z$  of the neural network prediction was taken as the objective of the minimum optimization, and the optimal process parameters were globally searched for by the PSO algorithm for the prediction model.

The particle swarm optimization algorithm was constructed based on the `ske PSO` toolkit of Python. The dimension of the search space `dim` was 6, population size `POP` was 20, the maximum number of iterations (`max_iter`) was 100, the inertia weight was 0.8, the learn-

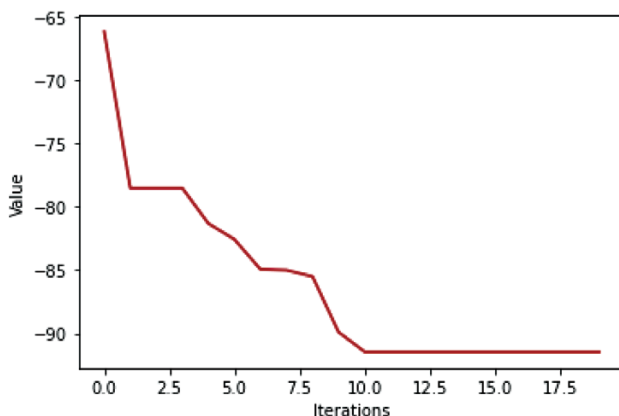


**Figure 3:** Optimal fitness value curve

ing factors  $C1 = C2$  were 0.5, and the constraints were: A (40–70 °C); B (190–220 °C); C (60–95 MPa); D (6–12

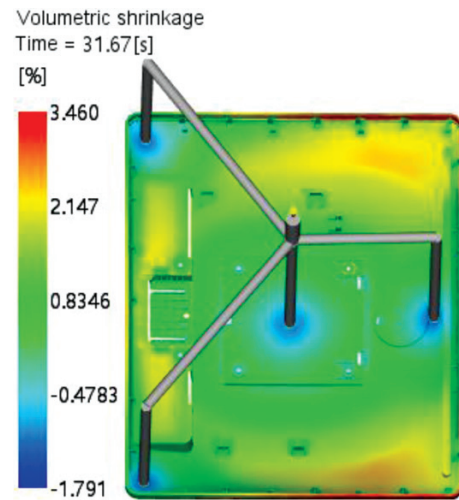


**Figure 4:** Optimized volumetric shrinkage

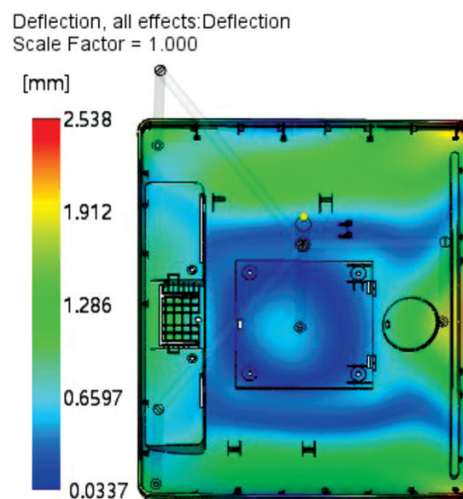


**Figure 5:** Optimized warpage deformation

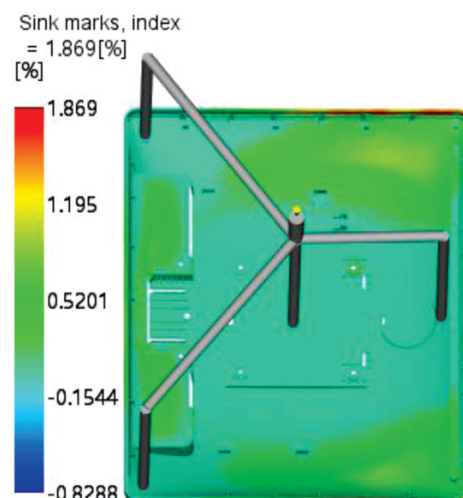


**Figure 6:** Optimized sink mark index

s); E (70–130 MPa); and F (0.9–1.3 s). The variation in the optimal fitness value was obtained as shown in **Figure 3**. After 10 iterations, the optimal fitness value of the PSO algorithm reached the minimum, and the optimized combination of process parameters obtained with the operation included a mold temperature of 40 °C, melt temperature of 190 °C, holding pressure of 95 MPa, pressure-holding time of 12 s, injection pressure of 70 MPa and injection time of 0.9 s. The optimized volumetric shrinkage was 3.9 %, the warpage deformation was 2.606 mm and the sink mark index was 2.2 % according to the numerical simulation based on Moldflow. The volumetric shrinkage was slightly reduced, the warpage deformation and the sink mark index were slightly increased, and the quality of the plastic part was not significantly improved.

The constraints were further adjusted as A (30–80 °C); B (180–230 °C); C (55–105 MPa), D (4–14 s); E (60–140 MPa); and F (0.7–1.5 s). The optimized process parameter combination was obtained again with the particle swarm algorithm; the mold temperature was 30 °C, the melt temperature was 180 °C, the holding pressure was 105 MPa, the pressure-holding time was 14 s, the injection pressure was 108.4 MPa, and the injection time was 0.7 s. Using Moldflow, the optimized volumetric shrinkage was reduced to 3.46 %, as shown in **Figure 4**. The warpage deformation decreased to 2.538 mm, as shown in **Figure 5**. The sink mark index dropped to 1.87 %, as shown in **Figure 6**. The three indicators were further reduced and the quality of the plastic parts was fully optimized.

## 4 CONCLUSION

1) Based on an orthogonal test and single-objective range analysis, the combination of process parameters that allows a single-objective optimization is determined, but the multi-objective optimization cannot be achieved at the same time.

2) The entropy weight was used to transform a multi-objective problem into a single-objective problem, obtaining the following results: the optimal process parameter combination was A2-B1-C1-D4-E1-F1, i.e., the volumetric shrinkage was 4.02 %, the warpage deformation was 2.573 mm, and the sink mark index was 2.14 %. The overall quality of the plastic part was further improved.

3) After the BP neural network fitting and PSO, further optimal process parameters were found, i.e., a mold temperature of 30 °C, a melt temperature of 180 °C, a holding pressure of 105 MPa, a pressure-holding time of 14 s, an injection pressure of 108.4 MPa, and an injection time of 0.7 s. The optimized volumetric shrinkage was reduced to 3.46 %, the warpage deformation was reduced to 2.538 mm, the sink mark index was reduced to 1.87 %, and the injection quality of the plastic part was optimized comprehensively.

## Acknowledgment

This work was sponsored by the Natural Science Foundation Program of the Fujian Province (2022J01609), Special Foundation for Science and Technology Innovation of the Fujian Agriculture and Forestry University (No.CXZX2020132B) and 2021 Fujian Province Young and Middle-Aged Teachers' Education and Research Project (No.JAT210819).

## 5 REFERENCES

- <sup>1</sup> R. Khavekar, H. Vasudevan, B. Modi, A comparative analysis of Taguchi methodology and Shainin system DoE in the optimization of injection molding process parameters, *IOP Conf. Ser.: Mater. Sci. Eng.*, 225 (2017) 1, doi:10.1088/1757-899X/225/1/012183
- <sup>2</sup> Y. Nie, H. M. Zhang, J. T. Niu, Optimization of the Injection Molding Process Parameters Based on Moldflow and Orthogonal Experiment, *Key Engineering Materials*, 561 (2013), 239–243, doi:10.4028/www.scientific.net/KEM.561.239
- <sup>3</sup> X. F. Li, H. B. Liu, Optimization of Injection Molding Process Parameters Based on Taguchi Design of Experiment, *Applied Mechanics and Materials*, 233 (2012) 11, 335–338, doi:10.4028/www.scientific.net/AMM.233.335
- <sup>4</sup> F. Wang, Z. L. Chen, Research on Process Optimization of Thin-Wall Plastics Injection Based on Moldflow and Orthogonal Experiment, *Advanced Materials Research*, 399–401 (2012), 1646–1649, doi:10.4028/www.scientific.net/AMR.399-401.1646
- <sup>5</sup> G. Xu, Z. T. Yang, Multiobjective optimization of process parameters for plastic injection molding via soft computing and grey correlation analysis, *The International Journal of Advanced Manufacturing Technology*, 78 (2015) 1–4, 525–536, doi:10.1007/s00170-014-6643-4
- <sup>6</sup> A. Sadeghi, A. Babakhani, S. M. Zabarjad, H. Mostajabodaveh, Use of grey relational analysis for multi-objective optimisation of NiTiCu shape memory alloy produced by powder metallurgy process, *Journal of Intelligent Material Systems and Structures*, 25 (2014) 16, 2093–2101, doi:10.1177/1045389X13517312
- <sup>7</sup> S. Q. Sun, S. K. Zhang, M. X. Huang, Optimization of injection molding process parameters based on signal-to-noise ratio and gray relational grade, *Journal of Plasticity Engineering*, 23 (2016) 1, 141–145, doi:10.3969/j.issn.1007-2012.2016.01.026
- <sup>8</sup> H. G. Zhang, Z. Y. Zhang, F. P. Wan, Y. Y. Liu, Q. X. Hu, Multi-objective optimization for DPVC process based on entropy-weight and RSM, *Computer Integrated Manufacturing Systems*, 20 (2014) 8, 1887–1895, doi:10.13196/j.cims.2014.08.zhangzhuangya.1887.9.20140811
- <sup>9</sup> X. Y. Lu, L. X. Fan, Y. Y. Ding, Multi-Objective Optimization of FDM Molding Process Parameters Combined With Entropy Weight TOPSIS, *Mechanical Science and Technology*, 4 (2017) 11, 1715–1721, doi:10.13433/j.cnki.1003-8728.2017.1113
- <sup>10</sup> T. Peng, H. Jun, W. D. Shi, Optimization of a Centrifugal Pump Used as a Turbine Impeller by Means of an Orthogonal Test Approach, *FDMP: Fluid Dynamics & Materials Processing*, 15 (2019) 2, 139–151, doi:10.32604/fdmp.2019.05216
- <sup>11</sup> H. Oktem, T. Erzurumlu, I. Uzman, Application of Taguchi optimization technique in determining plastic injection molding process parameters for a thin-shell part, *Materials & Design*, 28 (2007) 4, 1271–1278, doi:10.1016/j.matdes.2005.12.013
- <sup>12</sup> M. Cong, S. Zhang, D. Sun, K. Zhou, Optimization of Preparation of Foamed Concrete Based on Orthogonal Experiment and Range Analysis, *Frontiers in Materials*, 8 (2021), 488, doi:10.3389/fmats.2021.778173
- <sup>13</sup> K. Q. Zhong, Y. Xiao, X. Lu, J. Deng, Orthogonal Experimental Design and Range Analysis of TPCT Extraction of Coal Fire Heat,

- China Safety Science Journal, 31 (2021) 09, 135–141, doi:10.16265/j.cnki.issn1003-3033.2021.09.019
- <sup>14</sup> Z. H. Zou, Y. Yi, J. N. Sun, Entropy method for determination of weight of evaluating indicators in fuzzy synthetic evaluation for water quality assessment, Journal of Environmental Sciences, 18 (2006) 5, 1020–1023, doi:10.3321/j.issn:1001-0742.2006.05.032
- <sup>15</sup> C. Qiao, Y. Wang, C. H. Li, B. Q. Yan, Application of Extension Theory Based on Improved Entropy Weight Method to Rock Slope Analysis in Cold Regions, Geotechnical and Geological Engineering, 39 (2021) 6, 4315–4327, doi:10.1007/s10706-021-01760-9
- <sup>16</sup> Y. L. Cao, X. Y. Fan, Y. H. Guo, S. Li, H. Y. Huang, Multi-objective optimization of injection-molded plastic parts using entropy weight, random forest, and genetic algorithm methods, Journal of Polymer Engineering, 40 (2020) 4, 360–371, doi:10.1515/polyeng-2019-0326
- <sup>17</sup> Y. Kinouchi, G. Ohara, H. Nagashino, T. Soga, F. Shichijo, K. Matsumoto, Dipole source localization of MEG by BP neural networks, Brain Topography, 8 (1996) 3, 317–321, doi:10.1007/BF01184791
- <sup>18</sup> Z. Y. Song, S. M. Liu, X. X. Wang, Z. X. Hu, Optimization and prediction of volume shrinkage and warpage of injection-molded thin-walled parts based on neural network, The International Journal of Advanced Manufacturing Technology, 109 (2020) 3, 755–769, doi:10.1007/s00170-020-05558-6
- <sup>19</sup> M. L. Cong, S. S. Zhang, D. D. Sun, K. P. Zhou, Optimization of Injection Molding Process of Bearing Stand Based on BP Network Method, Transactions of Nanjing University of Aeronautics and Astronautics, 31 (2014) 2, 180–185, doi:10.3969/j.issn.1005-1120.2014.02.014
- <sup>20</sup> K. H. Fuh, S. B. Wang, Force modeling and forecasting in creep feed grinding using improved BP neural network, International Journal of Machine Tools and Manufacture, 37 (1997) 8, 1167–1178, doi:10.1016/S0890-6955(96)00012-0
- <sup>21</sup> D. Kramar, D. Cica, Predictive model and optimization of processing parameters for plastic injection moulding, Materiali in tehnologije / Materials and Technology, 51 (2017) 4, 597–602, doi:10.17222/mit.2016.129